

Individual formation parameters of charged point defects in ionic crystals: Silver chloride

R. A. Hudson, G. C. Farlow,* and L. M. Slifkin

*Department of Physics and Astronomy, University of North Carolina at Chapel Hill, Phillips Hall 039A,
Chapel Hill, North Carolina 27514*

(Received 20 January 1987)

The subsurface electric potential in oriented single crystals of silver chloride has been directly mapped out by a technique based on the equilibrium distribution of a very small concentration of a charged radiotracer. The potential was found to vary with depth according to the Gouy-Chapman solution of Poisson's equation, with screening lengths in the range 10–20 nm. The surfaces were all negative, relative to the deep interior, by 0.10–0.30 V, depending on temperature and surface orientation. The present results on the subsurface potential difference can be employed to resolve the Frenkel-pair formation enthalpy and entropy, as determined from transport measurements, into the formation enthalpies and entropies of the individual point defects comprising the pair. For the silver chloride (110) surface, for example, $G_v = 0.74$ eV and $G_i = 0.37$ eV at 150°C; the best values obtained to date for H_v , H_i , S_v , and S_i , are 0.77 eV, 0.70 eV, 0.79k, and 9.0k, respectively.

I. INTRODUCTION

Transport measurements in ionic crystals, whether the defects are of Schottky or Frenkel type, yield the enthalpy and entropy for the formation of the dominant defect pair, but cannot resolve these two parameters into the contributions from each of the components of the pair. This is because, in the intrinsic region of temperature, the concentration of defects in the bulk of the crystal depends on the total formation free energy of the complete pair; one component of the defect pair cannot be created in the bulk without also creating the other, charge-compensating component. The pair-formation free energy, however, and hence the enthalpy and entropy, may be further resolved into the formation enthalpies and entropies of the individual point defects, referred to a particular surface, if measurements of the potential difference Φ_s across the subsurface ionic space charge can be made. This resolution is possible because Φ_s depends on the difference between the formation free energies of the defects comprising the Frenkel or Schottky pair, whereas the transport properties give values for the sum. Knowledge of these individual defect-formation parameters would be very useful in furthering the understanding of surface and dislocation effects, especially in the technologically important oxides and other ceramics. In addition, the experimental determination of the individual defect-formation parameters becomes even more interesting when combined with the modern capabilities of calculating the separate defect enthalpies and entropies, using such techniques as the HADES code.

The dominant point defect in AgCl is the cation Frenkel pair, of which the interstitial is more mobile than the vacancy by a factor of several hundred. Therefore in the intrinsic region, the ionic conductivity is due mainly to migration of the interstitial. At lower temperatures, in the extrinsic region, the impurity-induced vacancies dominate. As a result of this clear separation of

the interstitial and vacancy transport processes, AgCl is one of the better understood ionic systems. Detailed analyses of ionic conductivity¹ have shown that for the formation of the Frenkel pair in AgCl, the enthalpy and entropy are $H_F = 1.47$ eV and $S_F = 9.8k$, respectively. Other, equally careful analyses of ionic conductivity^{2,3} have given values for H_F and S_F of 1.49 eV and 11.1k, respectively. In the present work, we have arbitrarily used the Corish-Jacobs values for H_F and S_F ; the differences between the sets of values obtained in the two analyses are negligible. However, although the free energy of formation of a Frenkel pair, G_F , is thus well known, the division of this free energy into contributions from the interstitial and the vacancy is not.

Frenkel was the first to point out that in an ionic crystal the components of a Frenkel or Schottky pair could be formed separately at jogs on the crystal surface,⁴ i.e., kinks in the steps of the surface terraces. Many of the same observations were made independently by Lehocvec.⁵ If these formation free energies are unequal, this ability to create or annihilate the components separately results in the production of a net ionic charge on the surface, and a compensating space-charge layer under the surface. (For recent reviews, see Tan⁶ and Hoyer.⁷) Thus, in the case of AgCl, if the free energy of formation of an interstitial is less than that of a vacancy ($G_i < G_v$), then a greater number of positive interstitials than negative vacancies will be injected, giving rise to a net negative surface charge. This surface charge is compensated by a near-surface region enriched in interstitials and depleted of vacancies. The equilibrium distribution of the point defects in this space-charge region is such as to screen the deep interior of the crystal from the surface charge. The resulting potential Φ_s of the surface, relative to the bulk, depends on the difference $G_i - G_v$. Thus, knowing the value of Φ_s and also G_F , which is equal to $G_i + G_v$, the pair-formation free energy can be resolved into these two components. Then, from the temperature dependences of G_i and G_v , one further ex-

pects to be able to resolve these free energies into formation enthalpies and entropies, where the entropy term arises from defect-induced changes in normal-mode frequencies.

Previous studies of the ionic space charge, measuring such properties as dielectric loss of microcrystals,⁸⁻¹⁰ thin-film conductivity,¹¹⁻¹⁴ and the contact potential of large crystals,¹⁵ have given values of Φ_s somewhat indirectly. For example, the thin-film conductivity studies measure the longitudinal conductance as a function of film thickness and temperature. With some simplifying assumptions, the surface potential may be inferred from the excess conductance that is attributed to the space-charge layers at the two types of interface of the supported film. The contact-potential experiment, on the other hand, is straightforward and relatively simple in principle, but difficulty arises in deducing the surface potential because some of the necessary parameters are not quantitatively known. Alternatively, since divalent impurities tend to segregate into the surface region, due to the negative electric potential, one expects that solute analysis, which has earlier been done by means of secondary-ion mass spectroscopy (SIMS), should give information about the space-charge effect.^{16,17} The space-charge layer, however, is very thin (≈ 10 nm) and can be grossly perturbed by the levels of doping often used in techniques such as SIMS. Hence, the resolution of these previous experiments was not adequate to provide quantitative values of Φ_s for the undoped crystal.

In contrast to these earlier studies, in the present work we have developed a radiotracer redistribution technique that *directly* maps the subsurface potential $\Phi(x)$ with a depth resolution of 0.5 nm and without significant perturbation of the defect distribution. The basic idea behind the technique is that a divalent cationic substitutional impurity has a net positive charge in the AgCl lattice. Therefore the equilibrium distribution of such an ion, at concentrations too low either to perturb the defect concentrations in the host system or to produce impurity-vacancy complexes, must vary with depth x as $\exp[-e\Phi(x)/kT]$. Hence, if a crystal can be sectioned parallel to the surface, on a scale small compared to the thickness of the space-charge layer (≈ 10 nm), and if the divalent-cation concentration of each section can be accurately determined, then the depth distribution of the cation probe gives the electric potential profile directly.¹⁸ High-specific-activity radiotracers of the divalent cation are used in this experiment because they provide the detection sensitivity needed at the very low concentration levels of ≤ 0.1 parts per million (ppm). Thus, the concentration of radioactivity contained in each section is proportional to the divalent-cation concentration at that depth, which is in turn a measure of the local electrostatic potential. From the resulting potential profile, the potential difference between bulk and surface is thereby measured, and the separate free energies of formation for the interstitial and vacancy may then be calculated.

For an analogous problem, that of a charged surface in an electrolyte, Gouy¹⁹ and Chapman²⁰ derived a quite general result for the distribution of mobile charges

which satisfies Poisson's equation and compensates the charged surface. The resulting shape of the distribution is independent of the details of the model (providing that all charges are mobile). Gouy and Chapman also gave an expression for the screening length, usually denoted by κ^{-1} , which depends only on the density of mobile charges, the temperature, and the dielectric coefficient.

From considerations of classical statistical mechanics for an intrinsic crystal (i.e., one in which the thermally produced defects predominate, and impurity-introduced defects may be neglected), one can write for the surface potential,

$$2e\Phi_s = G_i - G_v + kT \ln(2). \quad (1)$$

This result follows simply from the requirement that there be no net charge for large distances from the surface.²¹ Here, the last term is due to the fact that there are two interstitial sites per unit cell. This relation assumes only that the net density of surface charge is small compared to the total density of positive and negative jogs, an assumption which—it will be shown below—is not necessarily always valid. Substituting $G_i = G_F - G_v$ yields the expression

$$G_v = -e\Phi_s + [G_F - kT \ln(2)]/2. \quad (2)$$

In addition, the inverse Debye screening length κ^{-1} , which is a measure of the thickness of the space-charge region, is found to be given by

$$\kappa^2 = 8\pi e^2(n_i + CN)/\epsilon kT. \quad (3)$$

The expression in parentheses is just the concentration of positively charged defects in the bulk of the crystal; N is the density of cation or anion sites, C is the bulk ratio of divalent impurity cations to cation lattice sites, and n_i is the bulk concentration of silver interstitial ions.

In contrast to the simplicity of Eq. (2), which is expected to be valid only in the intrinsic range of temperature, the analysis of Φ_s to yield G_v and G_i in the extrinsic region of temperature should include possible effects of divalent impurities on the concentrations of point defects. Kliever and Koehler,^{22,23} on the basis of a space-charge model which supposes an unlimited supply of surface jogs, included the effect of charged impurities through the inverse Debye screening length κ^{-1} to obtain the relation

$$G_v = -e\Phi_s + kT \ln[8\pi N e^2 (\kappa^{-1})^2 / (\epsilon kT)]. \quad (4)$$

One assumption of the Kliever model which has been discussed in a set of papers by Blakely and co-workers^{24,25} and also by Macdonald,²⁶ is the availability of an adequate number of sources and sinks for the interstitials and vacancies at the crystal surface. Presumably these sources and sinks are the charged jog sites on surface steps because, except for the sign of the charge, point-defect exchange with the surface must not change the topography of the surface. If, in contrast to the assumption of the Kliever model, there are only a relatively small number of jogs, then once these sources of interstitials begin to be depleted, the subsurface electric po-

tential will be affected significantly. Other models,²⁴⁻²⁶ in which the density of jogs or surface states and the occupation of these sites are considered explicitly, show that the Kliewer model is only a limiting case, and that one must, in general, include an additional entropic term in the expression for G_v . This configurational term has the form of $-kT \ln(A)$, where A is the ratio of the number of unoccupied (i.e., negatively charged) jogs to that of the occupied (i.e., positively charged) jogs. Unfortunately, this ratio is not known experimentally for any real surface, and so the added complexity of the model does not readily lend itself to analysis of our data. Nevertheless, it will be seen below that comparison of surfaces of different orientation can be interpreted in terms of this notion.

II. EXPERIMENTAL PROCEDURE

The experiments reported in the present paper were all carried out on nominally pure (total solute content ≤ 1 ppm) single crystals of silver chloride. These specimens were taken from larger crystals grown from the melt by C. B. Childs, of the Department of Physics and Astronomy. Because AgCl is light sensitive, all sample-preparation and experimental procedures were carried out under safe-light conditions. Since Φ_s could well be a function of the surface orientation,²⁷ various oriented samples with the large, working surfaces having either a (100), (111), (110), or vicinal (i.e., not of simple Miller indices) orientation were cut from the large single-crystal boules. These samples, roughly 2 mm thick and with a broad cross-sectional area of about 3 cm², are then polished with a series of silicon carbide abrasive papers and fine alumina polishing powders (5.0, 0.3, and 0.05 μm). This procedure provides a smooth flat surface and minimizes the final dislocation density. The dislocation density must be made very small since each dislocation has its own space-charge region which would subsequently perturb the defect equilibrium distribution in the subsurface space-charge layer.

Handling of the sample in the course of the experiment requires that extreme care be taken to ensure that the working surface is neither contaminated nor mechanically damaged. In order to facilitate such delicate treatment, a length of chemically inert platinum wire is first attached to the sample edge by passing current through the wire until a small area of AgCl melts along the edge.

A final chemical polish is achieved by suspending the sample for several hours in a dilute aqueous NaCl solution. (Scanning electron micrographs showed that aqueous NaCl is indeed an isotropic, nonpitting etchant for AgCl, and that surfaces prepared by this procedure are quite smooth.) Once this polishing procedure is completed, each sample is sealed in an ampoule which has been evacuated and backfilled with ≈ 50 mm of chlorine gas. The sample is heated at $\approx 8^\circ\text{C}/\text{h}$ to 400°C (55°C below the melting point) in order to remove any residual strain from the previous cutting and polishing, and is then slowly cooled. The oxidizing atmosphere of chlorine converts any atomic silver, which may have

been photolyzed by the light from the torch used in sealing the ampoules, back into AgCl. This procedure produces a highly polished surface, with no visible strain inside the sample when viewed between crossed polaroids.

As described above, the electrostatic potential profile, an example of which is displayed in Fig. 1, is sensed by a determination of the distribution of the high-specific-activity radiotracer of a divalent cation. Since doping a sample of this size uniformly with suitable radiotracers would require an inconveniently large amount of radioactivity, a thin layer which typically contains 0.5 μCi of tracer is precipitated onto each broad, oriented surface and is diffused into the subsurface region to a diffusion length of about 5 μm . Apart from the near-surface space-charge region, the concentration profile of the diffused radiotracer has a Gaussian distribution, of which the first micrometer is uniform to within 2%. Since the thickness of the subsurface space-charge layer is less than 0.05 μm , the "bulk" radiotracer concentration appears flat on this scale. Actually, each crystal is doped with two different radiotracers, each at levels of about 0.1 ppm or less: (a) the divalent cation, which serves as the charged probe of the electric potential, and (b) radioactive ^{36}Cl , the distribution of which is not affected by the subsurface field, and the amount of which subsequently assayed in each section is a measure of the thickness of that cut. Chlorine-36 is a natural choice for such a depth gauge in AgCl because it has an extremely long half-life and an easily detectable β emission.

Manganese-54 was first chosen as the divalent potential probe tracer because its diffusion coefficient over the temperature range of interest is such as to allow its equilibrium distribution to be reached during an anneal of several weeks. In addition, the Mn^{2+} ion has a diffusion coefficient small enough at room temperature such that the quenched ^{54}Mn -concentration profile will not redistribute appreciably during the 30 minutes required for subsequent sectioning process. ^{54}Mn also has an easily detectable γ -ray emission, readily distinguished from the

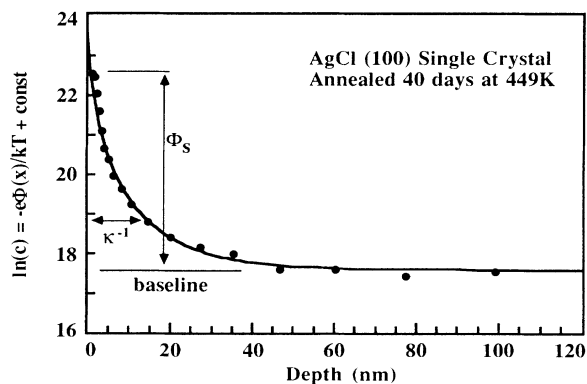


FIG. 1. Electric potential profile for AgCl (100) surface at 176°C . The local divalent tracer concentration is proportional to c . The curve shows the Gouy-Chapman fit, with inverse Debye screening length κ^{-1} . The measured potential difference, Φ_s , is the value used for the surface potential, rather than the extrapolated value, as justified in the text.

^{36}Cl radiation, and a convenient half-life of 300 days. As a check that any unsuspected chemical effects are not perturbing the electrostatic distribution, a second tracer, ^{51}Cr , is also used in some runs as the probe tracer.

Now that the samples have been doped with suitable radiotracers, they are each placed in a constant-temperature oven at various annealing temperatures. In earlier runs, the annealing was performed in air, but after discovering evidence of an in-diffusion of oxygen (especially at the higher temperatures), all later runs were made in helium. The samples are suspended in reusable ampoules such that no light is required to seal them, evacuated to 10^{-6} torr, and backfilled with ≈ 50 torr of helium for heat exchange. The annealing time must be sufficient for the low-mobility ^{54}Mn ions to reach the equilibrium subsurface depth distribution, a process much slower than bulk diffusion, because of the suppression of the concentration of cation vacancies near the surface. As a result of the increased time needed to achieve solute equilibrium, usually several weeks, it becomes very difficult to obtain the equilibrium distribution for annealing temperatures below about 60°C . Once equilibrium is finally established, the sample is quenched, thus "freezing in" the radiotracer distribution characteristic of the annealing temperature, which ranged from 25° to 300°C .

After quenching from the annealing temperature, the space-charge layer is sectioned by successively dipping the crystal into each of 20 beakers, each containing 11.8% aqueous NaCl, which acts as a slow, nonpitting solvent. Sections taken near the initial surface, where the dissolution rate is higher than normal²⁸ and where the impurity concentration varies strongly with depth, are taken in just a few seconds, in order to produce very thin cuts (≈ 0.5 nm). Sections taken toward the deep side of the space-charge region, where the impurity concentration varies slowly, involve dissolution times of about 2 min, yielding cut thicknesses of up to about 15 nm. The total thickness (≈ 100 nm) of the 20 layers is determined from the mass loss (≈ 0.2 mg) of the sample, which, since AgCl is nonhygroscopic, may be measured with an electronic microbalance. This mass-loss measurement is then used to calibrate the determination of the individual cut thicknesses obtained from measurement of the ^{36}Cl activity in each section. Then, the values of $\Phi(x)$ are obtained from the ^{54}Mn or ^{51}Cr activities and the individual cut thicknesses, making use of the classical statistical mechanics expression,

$$\ln[^{54}\text{Mn}] = -e\Phi(x)/(kT) + \text{const} . \quad (5)$$

This implies that a simple plot of the $\ln[^{54}\text{Mn}]$ versus depth will yield not only the spatial dependence of the electric potential but also the magnitude and sign of the potential difference Φ_s between the surface and the interior. Moreover, since the original Gaussian tracer profiles are very much deeper than the ≈ 15 -nm Debye length, this procedure can be repeated in a succession of further runs without the necessity of redoping the crystal or otherwise treating the surface.

In these experiments, no systematic dependence of the results on the specific activity of the tracers or on the

choice of ^{54}Mn or ^{51}Cr was observed. This suggests that the data are not significantly perturbed by any chemical effects or by the presence of unknown, nonradioactive impurities accompanying the tracer. The counting statistics were always accurate to within 5%, and usually to within 2%. Probably the largest sources of error in the experiment are fluctuations in the measured bulk concentration of probe tracer (presumably a result of local space charges due to the electrical effects of internal dislocations) and in the determination of the overall mass etched from the single-crystal sample. Fortunately, an error in the value of the total mass difference affects only the calibration of the depth scale and not the determination of the potential difference Φ_s , which depends only on the ratio of tracer concentrations at the surface and in the deep interior. In addition, any deviations from the expected Gouy-Chapman equilibrium distribution of probe tracer are most pronounced in the shape of the potential profile and not in the magnitude of Φ_s . Even the in-diffusion of oxygen, observed in the earlier air-annealed samples, seems to have altered only the near-surface shape of the solute distribution plot, without affecting the measured Φ_s . Thus, the measured Φ_s values, the accuracy of which seems to be limited only by uncertainties in the bulk base-line concentration of probe tracer, are more reliable than are our experimental values of the Debye screening length.

III. RESULTS

A. Shape of the potential profile

For measurements of the space-charge region when the equilibration annealing time was only a few days, the profile did not have the expected monotonic profile, but rather displayed an intermediate maximum between two minima. These intermediate maxima and minima are most likely due to the combination of initial vacancy fluxes and the spatially varying diffusivity of the probe tracer. For example, when a fresh space-charge defect distribution begins to develop, one expects a flux of vacancies, along with some divalent impurities, to the surface. Divalent impurities a bit further from the surface are attracted by the negative surface charge but the vacancy-depleted region causes the impurities to pile up, forming local maxima and minima in an otherwise monotonic profile. That these maxima and minima are indeed transient artifacts is demonstrated by the observation that when the annealing time is increased, the profile approaches the expected Gouy-Chapman form.

Another artifact of the experimental procedure occurred in the earlier runs when the samples were annealed in air. Those air-annealed profiles taken at the higher temperatures also did not have the expected Gouy-Chapman shape near to the surface, but instead showed a plateau for the first 5–20 nm. The thickness of the plateau increased with increasing annealing time, which suggests an in-diffusion of oxygen to form electrically neutral complexes with the divalent probe cations. This problem was readily eliminated in the later runs by annealing the specimens in ampoules which had provision for evacuation and subsequent backfilling with helium. In retrospect, however, comparison of runs

made in air and in helium shows that although the indiffusion of oxygen perturbs the profile shape, and hence, the measured value for the screening length, it does not significantly affect the measured value of Φ_s .

The results of a typical run for which the annealing time is long enough for establishment of an equilibrium profile, and for which the annealing atmosphere is helium rather than air, are shown in Fig. 1. The ^{54}Mn concentration is seen to be greatly enhanced at and near to the surface, relative to the bulk, implying a large and negative Φ_s . The depth resolution of the measurement is about 0.5 nm, and the overall fit to the Gouy-Chapman solution of Poisson's equation is seen to be excellent. Moreover, the screening length obtained from the fit (134 Å) is close to that expected from the known concentration of charged point defects in the bulk (183 Å for a crystal with 1-ppm divalent-impurity content and/or 151 Å for a 2-ppm crystal). However, although not apparent in Fig. 1, the first data point is usually found to be somewhat below the Gouy-Chapman curve. This appears to be a real effect, rather than an artifact. One possible explanation might involve a depth redistribution of the divalent probe tracer during the quenching and sectioning steps. This was checked by the use of a divalent chromium rather than a manganese tracer. Chromium has a significantly smaller diffusion coefficient than does manganese at room temperature, which would reduce any such redistribution. The deviation of the first point was found, however, to be independent of the choice of the probe tracer, and it therefore appears to be a real effect.

A likely explanation of this deviation is provided by calculations of the vacancy formation energies near the surface of an ionic crystal.²⁹ The results of atomistic computer simulations for a relaxed (001) surface of MgO show that near to the surface the vacancy energies of formation are a function of depth; moreover, they do not vary monotonically from the surface to the bulk but pass through a maximum at the second and third planes of atoms. Such a depth dependence would be expected to perturb measurably the equilibrium distribution of a probe tracer in the first cut or two. Although the computer simulation was performed for MgO, qualitatively similar behavior may well be found in other ionic systems, including the silver halides. Therefore, a more complete model of the space-charge region in AgCl might well require inclusion of defect energies of formation which are functions of the distance from the surface. Assuming then that this deviation of the first point is not an artifact, it follows that the correct value for the surface potential is obtained from the intersection of the experimental value of the divalent tracer profile with the surface, and not from the extrapolated Gouy-Chapman fit. Hence, our subsequent analyses use the measured Φ_s rather than an extrapolated Φ_s , from which the defect formation energies from the real surface are to be calculated.

B. Measured subsurface potential difference

The temperature range of the runs in this work is from 25 to 300°C. The $\approx 300^\circ\text{C}$ limit is set by the high

bulk diffusivity of the probe tracer at these temperatures, such that the underlying Gaussian profile (the bulk base line) steadily broadens with time, and thus a near-surface equilibrium distribution would never be obtained. At the other end of the temperature range, difficulties are encountered for annealing temperatures much below 100°C, because the extremely small diffusivity of the probe tracer in the vacancy-depleted region necessitates unreasonably long annealings. For AgCl crystals with (100) surfaces, we performed 18 early runs, for which the values of the screening length might have been perturbed by the presence of air, and then 21 later successful "clean" runs in helium. For (111) surfaces, there are 24 such early, "suspect" runs and 17 successful "clean" determinations. We have thus far also performed 10 successful "clean" runs for the (110) surface and another 6 "clean" runs for a "random" or vicinal surface.

In every case, the surface is found to be negative, relative to the bulk, at a potential Φ_s ranging from -0.1 to -0.3 V, depending on the temperature and surface orientation. Plots of the measured Φ_s versus temperature for the various surfaces are shown in Figs. 2, 3, and 4. The magnitudes of Φ_s for the (110) and the vicinal surfaces, as a function of temperature, are seen to be similar to one another, but to be somewhat larger, by about 20–30%, than those for the (100) or (111) surfaces. This difference may well be a reflection of the different densities of jogs on the two types of surface. Since well-developed (110) and vicinal surfaces are almost never found in nature, they must be high-energy surfaces and are therefore expected to be densely faceted and terraced; thus their jog densities should be very great. The (100) and (111) surfaces, on the other hand, are both observed in precipitated microcrystals of silver halides, indicating that they are of relatively low energy. Thus, although the (111) surface is not likely to be atomically flat, neither the (111) nor the (100) surfaces are expected to be highly terraced. Hence, unlike (110) and vicinal surfaces, they must have a relatively low density of charged surface jogs.

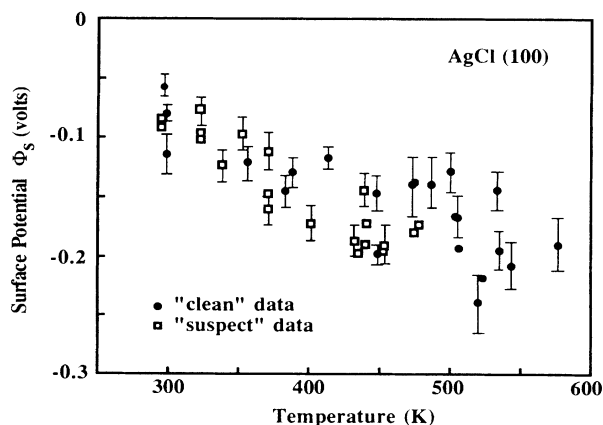


FIG. 2. Temperature dependence of the measured surface potential, Φ_s , for a (100) surface of AgCl. The "clean" and "suspect" data refer to annealings conducted in a helium or air atmosphere, respectively. Several typical error bars are shown.

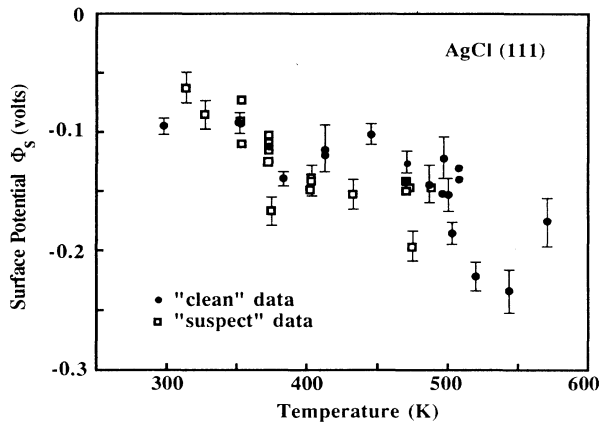


FIG. 3. Temperature dependence of the measured surface potential, Φ_s , for a (111) surface of AgCl. The "clean" and "suspect" data refer to annealings conducted in a helium or air atmosphere, respectively. Several typical error bars are shown.

C. Intrinsic analysis for free energies

For our crystals, the intrinsic region begins at about 150°C. In this case, if the density of surface jogs is great enough, as can be expected at least for the (110) and vicinal surfaces, one has the simple requirement for G_v as shown in Eq. (2). The results of applying this intrinsic relation to the Φ_s measurements for the (100) surface are shown in Fig. 5, as a plot of G_v versus temperature. A virtually identical plot results from the (111) data. The results for both the (110) and the vicinal surface are shown in Fig. 6; they are similar, although not identical, to those of Fig. 5. The values of G_i in each plot may be obtained from these figures by subtracting G_v from the total Frenkel-pair-formation free energy, G_F (i.e., $H_F = 1.47$ eV and $S_F = 9.8k$), shown as the upper dashed line. One sees that for all of the various surfaces, the resulting plots of G_v versus temperature are quite linear over the entire temperature range, with no apparent break between the extrinsic and intrinsic regions. It ap-

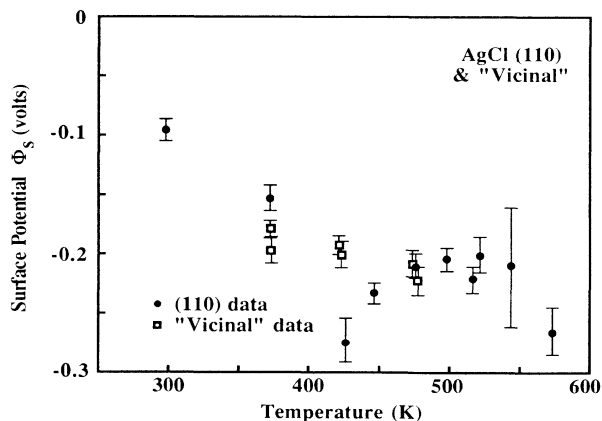


FIG. 4. Temperature dependence of the measured surface potential, Φ_s , for a (110) and "vicinal" surface of AgCl. All runs are performed in helium and several typical error bars are shown.

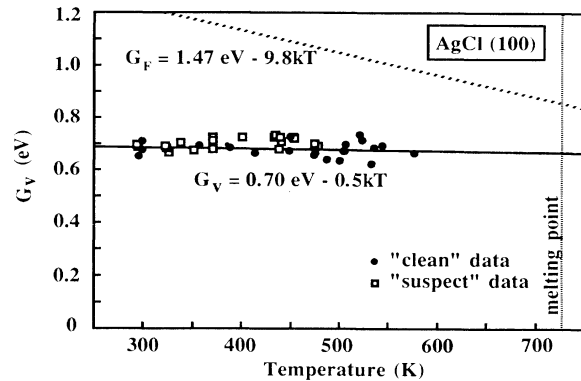


FIG. 5. Temperature dependence of G_v for a (100) surface of AgCl, obtained from the intrinsic relation. The "clean" and "suspect" data refer to annealings conducted in a helium or air atmosphere, respectively. For any particular temperature, the difference between G_F and G_v is G_i .

pears as though the defect concentration within the space-charge region is so large that the 1 ppm of background impurity produces little effect at temperatures much above room temperature. Earlier measurements of thin-film ionic conductivity⁹⁻¹² and contact potential¹³ also showed no evidence at all of such a break, and this anomaly thus appears to be real but unexplained. It is possible that the anomaly is also related to an inadequacy in the jog density, although the similarity between the (100) and (111) surfaces, on the one hand, and the (110) and vicinal surfaces, on the other, would seem to argue against this.

From these plots, noting that $G = H - TS$, and ignoring the uncertainty about the possibility of a jog saturation effect, one can not only obtain G_v and G_i for the various surface orientations, but, in addition, one can resolve these formation free energies into the separate enthalpies and entropies. The results are collected in Table I. It is interesting that these results indicate that the formation parameters depend only weakly on the surface orientation. Also, this analysis would indicate

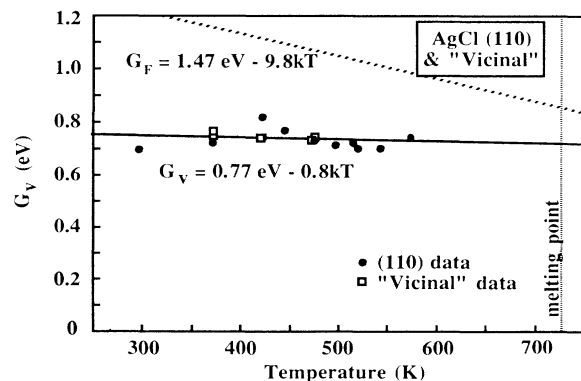


FIG. 6. Temperature dependence of G_v for a (110) and "vicinal" surface of AgCl, obtained from the intrinsic relation. For any particular temperature, the difference between G_F and G_v is G_i .

TABLE I. AgCl defect-formation parameters.

Surface	H_v (eV)	S_v/k	H_i (eV)	S_i/k
(100)	0.70	0.49	0.77	9.3
(111)	0.69	0.58	0.78	9.2
(110) and vicinal	0.77	0.79	0.70	9.0

that, whereas the formation enthalpy of the Frenkel pair is approximately evenly divided between H_v and H_i , the formation entropy seems to come primarily from the effect of the interstitial, rather than the vacancy, on the phonon frequencies. For the (100) and (111) surfaces, these conclusions are somewhat clouded by uncertainties as to whether these flat, low-energy surfaces do indeed have a high enough density of jogs to preclude jog saturation. For the (110) and vicinal surfaces, however, the jog density is expected to be quite high, and it would appear that the values of H and S are reliable. These results may perhaps represent the first quantitative resolution of pair formation parameters into the contributions from individual defects, along with a concurrent, similarly motivated study by Harris,³⁰ using contact-potential techniques, on sodium chloride.

IV. DISCUSSION

Ideally, the analysis of Φ_s to yield G_v and G_i should include possible effects of the background concentration of divalent impurities, which for our crystals is about 0.5–1 ppm, as determined from ionic-conductivity measurements. For this level of purity, any such effects would be negligible above about 150°C, but should become significant for annealing temperatures well below this temperature. As described above, Kliever and Koehler, using a model which supposes an unlimited supply of surface jogs, included the effect of impurities through the inverse Debye screening length κ^{-1} and obtained the relation given by Eq. (4). Unfortunately, the application of Eq. (4) to our data for the various surfaces employed was found to yield physically unacceptable results. An example is shown in Fig. 7 for the (100) sur-

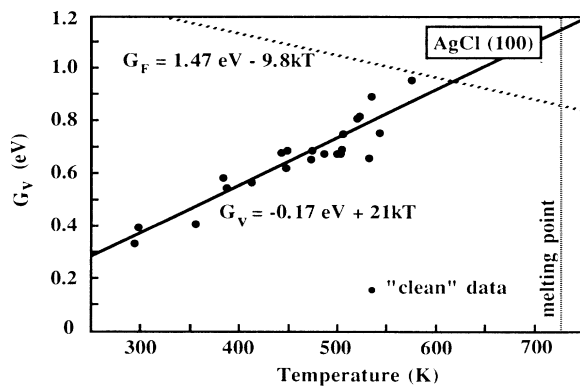


FIG. 7. Temperature dependence of G_v for a (100) surface of AgCl, as obtained from the Kliever-Koehler relation which includes the effect of divalent cationic impurities through κ^{-1} .

face, in which the plot of the derived G_v versus T gives a line corresponding to (a) a negative value of H_v (the vacancy formation enthalpy); (b) an unacceptably large and negative value for S_v [$-21k$, $-18k$, and $-12k$ for the (100), (111), and (110)-plus-vicinal surfaces, respectively]; and (c) a value of G_v that is greater than G_F , when extrapolated to higher temperatures. Moreover, in the intrinsic temperature range, the results of this analysis disagree strongly with those based on the simpler intrinsic relation of Eq. (2), which is expected to be valid at least for temperatures above 150°C.

There are several possible explanations for the observation that this analysis, in which the effect of divalent cations is accounted for in terms of κ^{-1} , seems to give unacceptable results. One possibility is that all of the surfaces have an inadequate number of jogs, although this would seem to be unlikely for the (110) and the vicinal surfaces. Another possibility is that the values obtained for the screening length in the present experiments are subject to large error. As mentioned above, an error in determination of κ^{-1} could arise from the fact that the calibration of the depth scale requires the total loss in mass of the crystal to be determined accurately. Any small sources of error, such as variations in absorbed water, could perturb the depth scale, although this would not affect the measured value of Φ_s . In addition, since dislocations within the space-charge region would have their own space charges, then the tracer profile may become distorted, which could also alter the deduced value of the screening length. Finally, of course, there is the possibility that the Kliever-Koehler model is not applicable for other, yet unknown, reasons.

One possible source of error may yet lie in the treatment of the surface charge in the Kliever-Koehler model. It is common to assume that the surface charge can be treated as being distributed uniformly. The charge, however, is located at discrete jogs, and if they are widely separated then the situation is inherently quite different from that of a uniform surface charge density for distances relatively close to the surface. Figure 8 is a schematic diagram illustrating this idea and how it would effect the depth profile measurements. For $\Phi_s = -0.1$ to -0.3 eV, and typical screening lengths of ≈ 15 nm, the charge density is computed to range from 10^{12} to 5×10^{13} e/cm², respectively. Since each jog has an effective charge of $e/2$, this corresponds to an excess density of negative jogs of from 2×10^{12} to 10^{14} cm⁻². This may be compared to the surface ion density, of the order of 10^{15} cm⁻². These densities of excess jogs correspond roughly to one excess negative jog for every 500–10 surface cations, respectively, at an average separation of 7–1 nm. For the larger average separations, corresponding to lower temperatures, this changes the

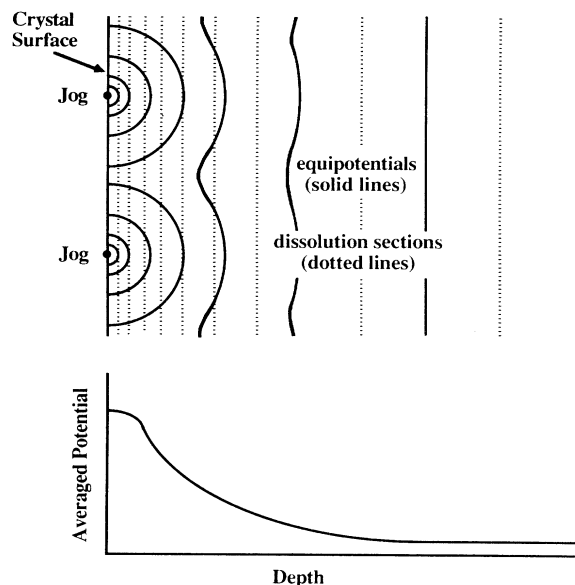


FIG. 8. Schematic diagram illustrating the possible effect of the discreteness of the jog density on the depth profile measurements. In a real crystal, the semicircular equipotentials would, of course, be distorted somewhat. This situation would perturb the values obtained for both κ^{-1} and Φ_s . It may also explain the consistently low first data point in tracer profiles.

picture of the defect distribution and the surface potential, since both of these properties will now vary spatially in directions parallel to the surface as well as perpendicular. This could drastically alter the derived screening lengths, with Φ_s becoming a sort of averaged surface potential. In addition, this effect provides an alternative explanation for the fact that the first point of the experimental tracer concentration profile is almost invariably below the Gouy-Chapman curve.

In a recent note,³¹ Baetzold and Hamilton have reanalyzed their earlier data¹¹ on the excess conductance of thin films of AgBr, now allowing for the temperature dependence of the screening length and using modern values of the Frenkel pair defect parameters.³ They now conclude that for the (111) surface of AgBr, H_i and H_v are nearly equal, and that the negative surface charge is due either to (a) an ionic relaxation at the surface, or (b) a formation entropy for the interstitial which greatly exceeds that of the vacancy. It is interesting that our results on AgCl are in excellent concordance with this latter interpretation. It thus appears that the negative surface potential on the silver halide is not due to a low value of H_i but, instead, to a high value of S_i .

These measurements of the formation parameters will also be useful in evaluating the interionic potentials developed for HADES-type simulations. Up to now, only the sums of the theoretically determined values for $(H_i + H_v)$ and $(S_i + S_v)$ could be tested by comparison with experiment. If there were any compensating errors, for example, in the theoretical S_v and S_i values, then this might not be apparent in comparing the sums.

Now, however, the theoretical and experimental values for the individual enthalpies and entropies can be compared with one another. Alternatively, since our experiment gives much more reliable values for G_i and G_v than for the individual enthalpies and entropies (which depend on the slope and the extrapolation of the G versus T plots), then a comparison between experimental and theoretical G_i and G_v values at a given temperature provides an alternative test which could expose any underlying compensation of errors in the comparisons of total pair enthalpy and pair entropy. Such theoretical calculations of the individual formation parameters in AgCl are currently underway.³²

In addition, there is some interest and value in repeating this experiment for AgBr. The intrinsic range extends to lower temperatures in AgBr than for AgCl, and this would make it possible to obtain intrinsic results over a much broader temperature range. Equally important, not only are the measured surface potentials expected to be larger in AgBr than in AgCl, but an appreciable difference in Φ_s for the (100) and (111) surfaces is expected from the results of thin-film conductivity¹¹⁻¹⁴ and dielectric-loss⁸⁻¹⁰ measurements. A further interesting extension of this experiment will be its application to NaCl, in order to compare the results with contact potential measurements,³⁰ and also because for this substance the interatomic potentials are better known than for the silver halides. The set of calculated point defect formation parameters for NaCl, including the entropies, is presently being refined by Harding, and an experimental comparison should be of some significance.³³

V. CONCLUSIONS

Although there are still some unanswered questions concerning the jog density, the screening, and the problems in applying the Kliever-Koehler analysis, several noteworthy conclusions can be drawn from the present experiment. This radiotracer technique for determining the near-surface divalent impurity profile has been shown to work remarkably well in AgCl and can be extended to other ionic materials. These profiles, obtained for the various crystallographic surfaces over a temperature range, show conclusively that a net negative surface charge exists on AgCl, that the space charge region contains an excess of interstitial silver ions and cationic divalent impurities, and they give quantitative values for the surface potential. The magnitude of the surface potential is found to increase monotonically with increasing temperature. From these results, the deduced values of G_v and G_i versus temperature also appear to be reliable in the intrinsic region, especially for those highly terraced surfaces for which the jog density is expected to be large. In addition, it is found that the silver interstitial and vacancy free energies of formation do not seem to be very dependent on the surface orientation. The results obtained to date indicate that, whereas the enthalpies of formation of the interstitial and the vacancy in AgCl are of comparable magnitude, the entropy of formation of the silver interstitial is much greater than that

for the cation vacancy. Finally, this technique appears to be readily generalizable to a variety of other substances in which the point defects carry an effective charge, such as other halides and many ceramic materials.

ACKNOWLEDGMENT

This research was supported by the National Science Foundation (Solid State Chemistry Program), under Grant No. DMR-85-01059.

-
- *Present address: Physics Department, Wright State University, Dayton, Ohio 45435.
- ¹J. Corish and P. Jacobs, *J. Phys. Chem. Solids* **33**, 1799 (1972).
- ²J. Aboagye and R. Friauf, *Phys. Rev. B* **11**, 1654 (1975).
- ³R. Friauf, in *The Physics of Latent Image Formation in Silver Halides*, edited by A. Baldereschi, W. Czaja, E. Tosatti, and M. Tosi (World Scientific, Singapore, 1984), p. 79.
- ⁴J. Frenkel, *Kinetic Theory of Liquids* (Oxford University Press, New York, 1946), p. 36.
- ⁵K. Lehovc, *J. Chem. Phys.* **21**, 1123 (1953).
- ⁶Y. Tan, *Prog. Solid State Chem.* **10**, 193 (1976).
- ⁷H. Hoyer, in *The Physics of Latent Image Formation in Silver Halides*, edited by A. Baldereschi, W. Czaja, E. Tosatti, and M. Tosi (World Scientific, Singapore, 1984), p. 151.
- ⁸H. Hoyer, *J. Appl. Phys.* **47**, 3784 (1976).
- ⁹M. Van Hulle and W. Maenhout-Van Der Vorst, *Phys. Status Solidi A* **44**, 229 (1977).
- ¹⁰F. Callens and W. Maenhout-Van Der Vorst, *Phys. Status Solidi A* **59**, 453 (1980).
- ¹¹R. Baetzold and J. Hamilton, *Surf. Sci.* **33**, 461 (1972).
- ¹²R. Baetzold, *J. Phys. Chem. Solids* **35**, 89 (1974).
- ¹³L. Brady, J. Castle, and J. Hamilton, *Appl. Phys. Lett.* **13**, 76 (1968).
- ¹⁴N. Starbov, A. Buroff, and J. Malinowski, *Phys. Status Solidi A* **38**, 161 (1976).
- ¹⁵S. Danyluk and J. Blakely, *Surf. Sci.* **41**, 359 (1974).
- ¹⁶Y. Tan, *Surf. Sci.* **61**, 1 (1976).
- ¹⁷B. Furman, G. Morrison, V. Saunders, and Y. Tan, *Photogr. Sci. Eng.* **25**, 121 (1981).
- ¹⁸G. Farlow, A. Blose, Sister J. Feldott, B. Lounsbury, and L. Slifkin, *Radiat. Eff.* **75**, 1 (1983).
- ¹⁹G. Gouy, *J. Phys. (Paris)* **4**, 457 (1910).
- ²⁰D. Chapman, *Philos. Mag.* **25**, 475 (1913).
- ²¹See, for example, R. Whitworth, *Adv. Phys.* **24**, 203 (1975).
- ²²K. Kliewer and J. Koehler, *Phys. Rev. A* **140**, 1226 (1965).
- ²³K. Kliewer, *J. Phys. Chem. Solids* **27**, 705 (1966).
- ²⁴R. Poeppele and J. Blakely, *Surf. Sci.* **15**, 507 (1969).
- ²⁵J. Blakely and S. Danyluk, *Surf. Sci.* **40**, 37 (1973).
- ²⁶J. R. Macdonald, D. Franceschetti, and A. Lehnen, *J. Chem. Phys.* **73**, 5272 (1980).
- ²⁷L. Slifkin, *J. Phys. (Paris) Colloq.* **34**, C9-247 (1973).
- ²⁸L. Cain, N. Daniele, J. Lee, and L. Slifkin, *J. Phys. (Paris) Colloq.* **41**, C6-106 (1980).
- ²⁹D. Duffy, J. Hoare, and P. Tasker, *J. Phys. C* **17**, L195 (1984).
- ³⁰L. B. Harris, *Cryst. Lattice Defects Amorph. Mater.* (to be published).
- ³¹R. Baetzold and J. Hamilton, *Surf. Sci.* **179**, L85 (1987).
- ³²J. Corish and P. Jacobs (private communication).
- ³³J. Harding (private communication).